Front. Phys. 11(2), 114401 (2016)
DOI 10.1007/s11467-015-0548-z

RESEARCH ARTICLE

Interface-facilitated energy transport in coupled Frenkel–Kontorova chains

Rui-Xia Su[1], Zong-Qiang Yuan[2], Jun Wang[3,*], Zhi-Gang Zheng[4,†]

[1] *Department of Physics and the Beijing–Hong Kong–Singapore Joint Centre for Nonlinear and Complex Systems (Beijing), Beijing Normal University, Beijing 100875, China*

[2] *Science and Technology on Plasma Physics Laboratory, Research Center of Laser Fusion, China Academy of Engineering Physics, Mianyang 621900, China*

[3] *Key Laboratory of Enhanced Heat Transfer and Energy Conservation (Ministry of Education), College of Environmental and Energy Engineering, Beijing University of Technology, Beijing 100124, China*

[4] *College of Information Science and Engineering, Huaqiao University, Xiamen 361021, China*

*Corresponding authors. E-mail: *jwang@bjut.edu.cn, †zgzheng@hqu.edu.cn*

Received November 5, 2015; accepted December 17, 2015

The role of interface couplings on the energy transport of two coupled Frenkel–Kontorova (FK) chains is explored through numerical simulations. In general, it is expected that the interface couplings result in the suppression of heat conduction through the coupled system due to the additional interface phonon–phonon scattering. In the present paper, it is found that the thermal conductivity increases with increasing intensity of interface interactions for weak inter-chain couplings, whereas the heat conduction is suppressed by the interface interaction in the case of strong inter-chain couplings. Based on the phonon spectral energy density method, we demonstrate that the enhancement of energy transport results from the excited phonon modes (in addition to the intrinsic phonon modes), while the strong interface phonon–phonon scattering results in the suppressed energy transport.

Keywords interface couplings, energy transport, heat conduction, phonon-phonon scattering, Frenkel–Kontorova (FK) chains, excited phonon modes, phonon spectral energy density

PACS numbers 44.10.+i, 63.20.Ry, 63.22.-m, 05.60.-k

1 Introduction

Recent years have witnessed an increasing number of studies on the thermal transport properties of nanostructured materials because understanding heat transfer at the nanoscale is of growing importance in the development of energy-conversion applications and the thermal management of microelectronic and optoelectronic devices [1–12]. Previous studies have all focused on a single free-standing nanostructure, such as isolated silicene [13–15], carbon nanotubes [16–21], graphene [22–26], and nanoporous Si [27]. However, it is inevitable that most nanostructures have to be supported or surrounded by environmental materials in practical applications, and the heat-transfer process may be significantly affected by the interface. Usually, the scattering of phonons at interfaces leads to a decreased phonon mean free path and suppressed thermal conductivity [28–30]. However, recent experimental and numerical results demonstrate that contact with a substrate counterintuitively enhances the thermal conductivity through double-wall carbon nanotubes [31], supported graphene [32], supported silicene structures [33], and a bundle of nanoribbons [34]. Therefore, the interface effect can improve the thermal conductivity under certain conditions. However, a comprehensive theoretical explanation of this counterintuitive physical phenomenon is still lacking.

In 1938, Frenkel and Kontorova first proposed the FK model to study surface phenomena [35]. Despite the deceptively simple form of the model, it has been applied in a wide variety of physical systems, such as adsorbed monolayers, Josephson junctions, and DNA denaturation [36]. In condensed-matter physics and nonlinear physics, FK chains are also widely used to depict the heat conduction and phonon transport process of real materials [37–46]. Thus, we adopt a coupled FK chain model as a simplified working bench of the coupled nanostructures

and investigate the effect of interface couplings on the phonon transport process.

In the present paper, we employ numerical simulations to elucidate the thermal transport mechanisms of two coupled FK chains. It is found that the heat flow through the interacting FK chains vary nonlinearly with respect to the interface coupling intensity. For weak interface interactions, the energy transport is enhanced by the interface couplings, while for strong interface couplings, the heat flux is suppressed by the interface interaction. Based on the phonon spectral energy density (SED) method [19, 47–49], we obtained exact knowledge of the phonon spectra. By combining phonon band theory with numerical simulations to analyze the phonon spectra, we found that the enhancement of heat conduction mainly results from the additionally excited phonon modes, while strong interface phonon scattering leads to the suppression of thermal transport through strongly coupled FK chains.

2 Model of coupled FK chains

In this study, we investigate heat conduction in two coupled FK chains with linear inter-chain coupling strength k_c (see Fig. 1). The Hamiltonian of the entire system is

$$H = H_1 + H_2 + H_c, \tag{1}$$

$$H_n = \sum_{j=1}^{N}\left[\frac{{p_n^j}^2}{2m_n} + \frac{k_n}{2}(x_n^i - x_n^{j-1})^2 - \frac{V_n}{(2\pi)^2}\cos(2\pi x_n^j)\right], \quad \text{for } n = 1, 2, \tag{2}$$

$$H_c = \sum_j\left[\frac{k_c}{2}(x_2^j - x_1^j)^2\right]. \tag{3}$$

Here, H_1 and H_2 are the Hamiltonians of chain-1 and chain-2, respectively, and H_c denotes the Hamiltonian of the interfacial coupling term. Further, x_n^j and p_n^j are the relative displacement and momentum of the j-th atom in the n-th chain, respectively, and m_n, k_n, and V_n represent the mass, harmonic coupling constant, and strength of the on-site potential of chain n, respectively. For simplicity, we set $m_1 = m_2 = 1.0$, $k_1 = k_2 = 1.0$, and $V_1 = V_2 = 1.0$.

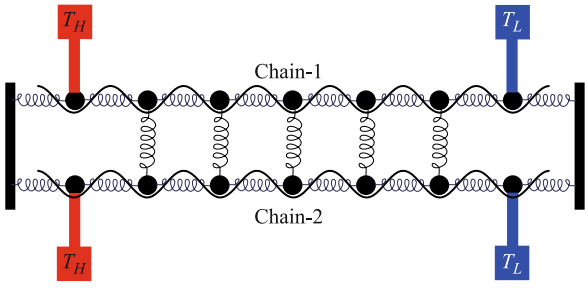

Fig. 1 Schematics of the coupled FK chains.

Fixed boundary conditions are adopted in nonequilibrium molecular dynamics (NEMD) simulations and two Nose–Hoover thermostats [50, 51] at $T_H = 0.06$ and $T_L = 0.04$ are applied on the first and last particle of each chain, respectively. The size of each lattice is set to be $N = 50$. In our simulations, the equations of motion are integrated using a fourth-order Runge–Kutta algorithm with a small time step of 0.01 [52]. After performing simulations for a sufficiently long time (the total integration is for 10^9 time steps), the system reaches a stationary state in which the heat flux is constant along the longitudinal direction of lattices. The local heat flux is defined by $J_n = \langle p_n^j \partial V_n'/\partial x_n^j\rangle$ based on the continuity equation, where V_n' denotes intra-chain interactions and $V_n' = \frac{k_n}{2}(x_n^j - x_n^{j-1})^2$ in this paper.

3 Dependence of heat flux on intensity of interface couplings

Figure 2(a) shows the dependence of heat flux on the inter-chain couplings k_c, where J_1, J_2, and J_t ($J_t = J_1 + J_2$) denote the heat fluxes of chain-1, chain-2, and the total heat flux, respectively. Because chain-1 and chain-2 are identical, J_1 should be equal to J_2 (thus, we only analyze the phonon-transport properties of chain-1 below). Figure 2(a) clearly shows that the heat flux increases with increasing k_c for weak interface couplings. The heat flux reaches its maximum at an intermediate strength of the inter-chain couplings. When k_c is further increased, the heat current decreases monotonously, which indicates that heat conduction is suppressed by the strong interfacial coupling. Considering the scale dependence of the thermal conductivity of FK chains [36, 45, 53, 54] (nanomaterials such as carbon nanotubes and graphene also show a certain scale dependence [56, 56]),

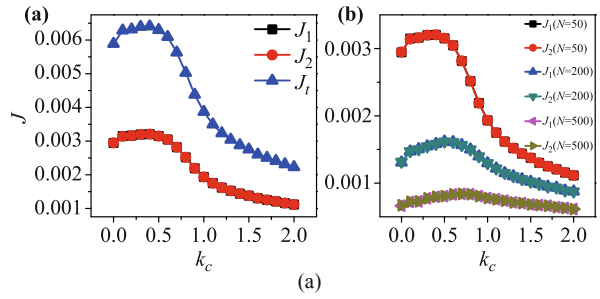

Fig. 2 **(a)** Dependence of the heat flux of coupled FK chains on the inter-chain coupling strength k_c; **(b)** Heat flux of different system sizes $N = 50, 200, 500$. J_1 and J_2 denote the heat flux of chain-1 and chain-2, respectively. J_t is the total heat flux of the coupled system.

we plot the the effect of size on this phenomenon in Fig. 2(b). The results show that the nonlinear dependence of heat conductivity on the intensity of interface coupling is size-insensitive. Thus, it is concluded that the heat conduction through two interacting FK chains can be manipulated by varying the strength of inter-chain couplings.

4 Analysis and discussion on the mechanism of heat-conductivity variation

To understand the underlying mechanism of the enhancement or suppression of thermal conductivity for two coupled FK chains, we calculate the phonon dispersion relation by using the SED method [19, 47–49]. The SED method can predict fully anharmonic phonon properties by using particle velocities obtained from the numerical simulations as follows:

$$\Phi_n(\omega,q)=\frac{m_n}{4\pi\tau_0 N}\times\left|\int_0^{\tau_0}\sum_{j=1}^{N}p_n^j\exp(\mathrm{i}2\pi\frac{j}{N}q-\mathrm{i}\omega t)\mathrm{d}t\right|^2, \quad (4)$$

where ω and $Q=2\pi q/(aN)=2\pi q/N$ ($q=-\frac{N}{2}$, $-\frac{N}{2}+1,...,\frac{N}{2}-1$, $\frac{N}{2}$, and the lattice constant a is set to be $a=1$) are the phonon frequency and wavevector, respectively, a is the equilibrium distance of adjacent atoms in chains, and i and τ_0 are the imaginary unit and total time of calculation, respectively. It is noted that the SED method is based on the equilibrium MD simulations; therefore, we must calculate SED under the periodic boundary condition and the equilibrium state at $T=(T_H+T_L)/2=0.05$ in the numerical simulations.

Figure 3 shows the SED pattern with different inter-chain couplings: (a) without inter-chain interactions ($k_c=0.0$), (b) weak inter-chain interactions ($k_c=0.13$), (c) moderate inter-chain interactions ($k_c=0.3$), and (d) strong inter-chain interactions ($k_c=2.0$). As the parameters of chains 1 and 2 are identical, their SED patterns should be identical; therefore, we only show the SED patterns of chain-1 here. As shown in Fig. 3, with increasing interface couplings, more additional phonon modes are excited, and meanwhile, the high-frequency phonon band shows an upward shift. When the strength of inter-chain couplings is sufficiently high, more side peaks (the messy bright lines in SED patterns) emerge, which implies strong phonon scattering.

At the low-temperature regime, the particles are confined at the bottom of the on-site potential owing to the small kinetic energy. Thus, the corresponding equation of motion of the coupled FK chians can be expressed as

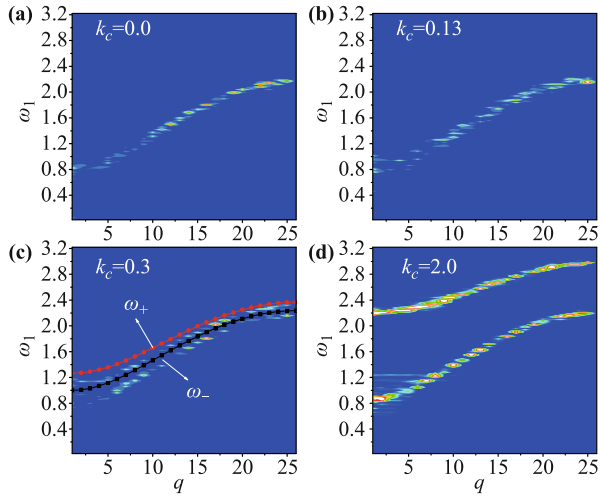

Fig. 3 Contour plot of phonon SED of chain-1 with different inter-chain couplings: **(a)** $k_c=0.0$, **(b)** $k_c=0.13$, **(c)** $k_c=0.3$, and **(d)** $k_c=2.0$. The contour plots are the results by SED method and the red and black dotted lines are the analytical result.

$$m\ddot{x}_1^j=k_1(x_1^{j+1}+x_1^{j-1}-2x_1^j)-k_c(x_1^j-x_2^j)-V_1x_1^j, \quad (5)$$

$$m\ddot{x}_2^j=k_2(x_2^{j+1}+x_2^{j-1}-2x_2^j)-k_c(x_2^j-x_1^j)-V_2x_2^j. \quad (6)$$

By setting the trial solutions in the forms $x_1^j=A_1e^{i(\omega t-jaQ)}=A_1e^{i(\omega t-jQ)}$ and $x_2^j=A_2e^{i(\omega t-jaQ)}=A_2e^{i(\omega t-jQ)}$ and by substituting them into Eqs. (5) and (6), we obtain the following:

$$(-m\omega^2-2k_1\cos Q+2k_1+k_c+V_1)A_1-k_cA_2=0, \quad (7)$$

$$(-m\omega^2-2k_2\cos Q+2k_2+k_c+V_2)A_2-k_cA_1=0. \quad (8)$$

The above equations can be regarded as linear homogeneous equations with unknowns A_1 and A_2, and the existence condition of the traveling-wave solution can be given as

$$\begin{vmatrix} C_1 & -k_c \\ -k_c & C_2 \end{vmatrix}=0,$$

where $C_1=-m\omega^2-2k_1\cos Q+2k_1+k_c+V_1$, $C_2=-m\omega^2-2k_2\cos aQ+2k_2+k_c+V_2$, and they satisfy the following relation:

$$C_1\times C_2-k_c^2=0. \quad (9)$$

The solution of Eq. (9) is

$$\omega_\pm^2=\frac{2(k_1+k_2)\sin^2\frac{Q}{2}+k_c+V}{m}\pm\frac{\sqrt{4(k_1-k_2)^2\sin^4\frac{Q}{2}+k_c^2}}{m}. \quad (10)$$

As $k_1=k_2$,

$$\omega_\pm^2=\left(4k_1\sin^2\frac{Q}{2}+V+k_c\pm k_c\right)/m. \quad (11)$$

Here, ω_+ and ω_- denote the high-frequency and low-frequency phonon modes, respectively. The analytical phonon dispersion relations are plotted in Fig. 3(c) by red and black dotted lines, and they are in qualitative agreement with the result obtained using the SED method. It is worth noting that the phonon frequency in the analytical result is shifted upward relative to the SED patterns, which can be ascribed to the contribution from the nonlinearity of the on-site potential.

Now, we analyze the mechanism of thermal-conductivity enhancement. The relaxation-time approximation of the Boltzmann transport equation approach yields the formula of thermal conductivity [47]:

$$\kappa = \sum_{Q}\sum_{\gamma} c_{ph} v_g^2(Q,\gamma)\tau(Q,\gamma), \tag{12}$$

where c_{ph} is the specific heat of the phonon, Q is the wave vector, γ denotes the phonon branch, $v_g(Q,\gamma) = \partial\omega/\partial Q$ is the group velocity of the phonon, and $\tau(Q,\gamma)$ is the phonon lifetime. In the classical limit, the phonon specific heat, c_{ph}, could be considered a constant. The two summations in Eq. (12) include all phonon modes.

The spectral energy density is a function of wave vector and frequency. Moreover, SED is a highly peaked function that should satisfy a Lorenzian distribution, and the peaks are centered at values of wave vector Q ($Q = 2\pi q/N$) and frequency ω at which phonons exist. Thus, we are able to confirm the phonon modes by drawing the SED peaks in the entire frequency range with a given Q. The full phonon spectra obtained in this manner are shown in Fig. 4, where ω_{1-} and ω_{1+} denote the low-frequency phonon branch and high-frequency phonon branch of chain-1, respectively. From Fig. 4(a), it is seen that the low-frequency phonon branch ω_- remains invariant with varying k_c. In the above expression of analytical dispersion relations, Eq. (11), it is also found that ω_- is independent of k_c. Actually, ω_- produces the exact phonon spectra for the corresponding single freestanding FK chain; thus, ω_- can be viewed as the intrinsic phonon branch, and the phonon group velocity does not vary with interface interactions. On the other hand, the phonon scattering originating from weak interface couplings is too weak to affect the phonon transport significantly at low k_c; i.e., the influence of inter-chain couplings on the mean free time or the mean free path of intrinsic phonons can be ignored. Therefore, for low k_c, the contribution of the intrinsic phonon branch to the total thermal conductivity does not change apparently with varying interface interactions.

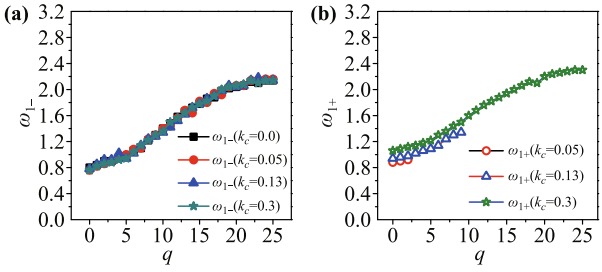

Fig. 4 Phonon SED peaks for the chain-1.

From Fig. 3 and Fig. 4(b), it can be seen that an increasing number of phonon modes of the high-frequency phonon branch ω_{1+} are excited with increasing k_c, and they emerge one by one with increasing wave vectors. For example, for $k_c = 0.05$, only the modes from $q = 0$ to $q = 2$ are excited, while for $k_c = 0.3$, the phonon modes of the entire high-frequency branch are fully excited. This implies that more phonons contribute to the energy-transport process of the coupled FK chains as k_c increases. This effect can also be seen from Eq. (12), in which more terms are involved in the summation operation with increasing k_c; thus, the thermal conductivity of the coupled system increases with increasing inter-chain couplings. It is noted that the excited high-frequency phonon branch slowly shifts upward with increasing k_c, as shown in Fig. 3, which leads to a smaller phonon group velocity and accordingly a suppression effect on the thermal transport. However, for low k_c, the shift of the high-frequency phonon branch is very weak, as shown in Fig. 4(b), and does not significantly influence the energy transport. Therefore, the dominant effect of the phonon excitation results in the thermal-transport enhancement of coupled system.

In the regime of strong interfacial couplings, the emergence of side peaks (messy bright lines) in the SED patterns in Fig. 3(d) indicates strong phonon scattering due to the large interfacial couplings. To demonstrate this in more detail, we present in Fig. 5 the SED distribution of the coupled FK chains with variation in frequency when $q = 3$. It is quite clear that many small thorns of side energy peaks appear for strong inter-chain couplings ($k_c = 4$), further illustrating the strong interface phonon scattering, which results in the reduced phonon lifetime; consequently, the thermal transport through

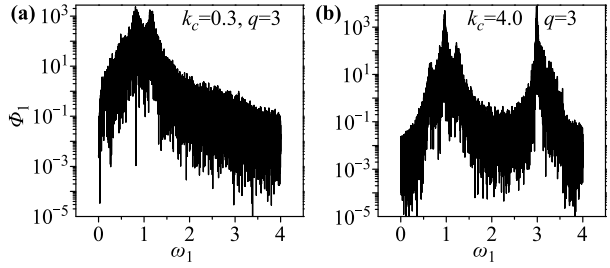

Fig. 5 Dependence of the energy density on the frequency while $q = 3$. Energy-density distributions of chain-1 for **(a)** $k_c = 0.3$ and **(b)** $k_c = 4.0$.

strongly coupled FK chains is suppressed by strong interface interactions.

5 Conclusions

In conclusion, we have investigated the effect of the interface couplings on the thermal transport of the coupled FK chains. It is found that the heat flux can reach a maximum on varying the strength of inter-chain couplings. In the regime of weak inter-chain couplings, the thermal transport can be enhanced by increasing the strength of interface interactions. However, for strong inter-chain couplings, heat flux is suppressed by the interface interaction. The analysis of the phonon SED patterns demonstrates that the emergence of additionally excited phonon modes is the primary mechanism for the enhancement of thermal transport for weak interface interactions, while strong interface phonon scattering leads to the the suppressed heat conduction through strongly coupled FK chains. For real applications, interface interactions always exist in nature. The results of the present study pave the way for manipulating the energy transport of nanoscaled materials, which is necessary for designing thermal devices.

Acknowledgements This work was partially supported by the National Natural Science Foundation of China (Grant Nos. 11475022, 51306004, and 11075016), the Doctoral Program of Higher Education of China (Grant No. 20131103120018), the Ri-Xin Talents Project of Beijing University of Technology (Grant No. 2015-RX-05), and the Scientific Research Funds of Huaqiao University.

References

1. A. I. Hochbaum, R. Chen, R. D. Delgado, W. Liang, E. C. Garnett, M. Najarian, A. Majumdar, and P. Yang, Enhanced thermoelectric performance of rough silicon nanowires, *Nature* 451(7175), 163 (2008)
2. M. Losego, M. E. Grady, N. R. Sottos, D. G. Cahill, and P. V. Braun, Effects of chemical bonding on heat transport across interfaces, *Nat. Mater.* 11(6), 502 (2012)
3. C. Yan, J. Cho, and J. Ahn, Graphene-based flexible and stretchable thin film transistors, *Nanoscale* 4(16), 4870 (2012)
4. G. J. Hu and B. Y. Cao, Thermal resistance between crossed carbon nanotubes: Molecular dynamics simulations and analytical modeling, *J. Appl. Phys.* 14(22), 224308 (2013)
5. R. Guo and B. Huang, Approaching the alloy limit of thermal conductivity in single-crystalline Si-based thermoelectric nanocomposites: A molecular dynamics investigation, *Sci. Rep.* 5, 9579 (2015)
6. R. Guo, X. Wang, and B. Huang, Thermal conductivity of skutterudite $CoSb_3$ from first principles: Substitution and nanoengineering effects, *Sci. Rep.* 5, 7806 (2015)
7. J. S. Wang, B. K. Agarwalla, H. Li, and J. Thingna, Nonequilibrium Green's function method for quantum thermal transport, *Front. Phys.* 9(6), 673 (2014)
8. N. P. Dasgupta and P. Yang, Semiconductor nanowires for photovoltaic and photoelectrochemical energy conversion, *Front. Phys.* 9(3), 289 (2014)
9. S. Li, Y. F. Dong, D. D. Wang, W. Chen, L. Huang, C. W. Shi, and L. Q. Mai, Hierarchical nanowires for high-performance electrochemical energy storage, *Front. Phys.* 9(3), 303 (2014)
10. N. Liu, W. Li, M. Pasta, and Y. Cui, Nanomaterials for electrochemical energy storage, *Front. Phys.* 9(3), 323 (2014)
11. Z. Liu and B. Li, Heat conduction in simple networks: The effect of interchain coupling, *Phys. Rev. E* 76(5), 051118 (2007)
12. Z. Liu, X. Wu, H. Yang, N. Gupte, and B. Li, Heat flux distribution and rectification of complex networks, *New J. Phys.* 12(2), 023016 (2010)
13. E. Scalise, M. Houssa, G. Pourtois, B. van den Broek, V. Afanas'ev, and A. Stesmans, Vibrational properties of silicene and germanene, *Nano Res.* 6(1), 19 (2013)
14. H. P. Li and R. Q. Zhang, Vacancy-defect–induced diminution of thermal conductivity in silicene, *Europhys. Lett.* 99(3), 36001 (2012)
15. Q. X. Pei, Y. W. Zhang, Z. D. Sha, and V. B. Shenoy, Tuning the thermal conductivity of silicene with tensile strain and isotopic doping: A molecular dynamics study, *J. Appl. Phys.* 114(3), 033526 (2013)
16. J. Shiomi and S. Maruyama, Molecular dynamics of diffusive-ballistic heat conduction in single-walled carbon nanotubes, *Jpn. J. Appl. Phys.* 47(4), 2005 (2008)
17. J. Hone, M. Whitney, C. Piskoti, and A. Zettl, Thermal conductivity of single-walled carbon nanotubes, *Phys. Rev. B* 59(4), R2514 (1999)
18. S. Berber, Y. K. Kwon, and D. Tomanek, Unusually high thermal conductivity of carbon nanotubes, *Phys. Rev. Lett.* 84(20), 4613 (2000)
19. J. Shiomi and S. Maruyama, Non-Fourier heat conduction in a single-walled carbon nanotube: Classical molecular dynamics simulations, *Phys. Rev. B* 73(20), 205420 (2006)
20. C. Yu, L. Shi, Z. Yao, D. Li, and A. Majumdar, Thermal conductance and thermopower of an individual single-wall carbon nanotube, *Nano Lett.* 5(9), 1842 (2005)
21. B. Y. Cao and Q. W. Hou, C. Bing-Yang, and H. Quan-Wen, Thermal conductivity of carbon nanotubes embedded in solids, *Chin. Phys. Lett.* 25(4), 1392 (2008)
22. A. A. Balandin, S. Ghosh, W. Bao, I. Calizo, D. Teweldebrhan, F. Miao, and C. N. Lau, Superior thermal conductivity of single-layer graphene, *Nano Lett.* 8(3), 902 (2008)
23. A. A. Balandin, Thermal properties of graphene and nanostructured carbon materials, *Nat. Mater.* 10(8), 569 (2011)

24. D. L. Nika, E. P. Pokatilov, A. S. Askerov, and A. A. Balandin, Phonon thermal conduction in graphene: Role of Umklapp and edge roughness scattering, *Phys. Rev. B* 79(15), 155413 (2009)
25. K. Saito, J. Nakamura, and A. Natori, Ballistic thermal conductance of a graphene sheet, *Phys. Rev. B* 76(11), 115409 (2007)
26. Z. Q. Ye, B. Y. Cao, W. J. Yao, T. Feng, and X. Ruan, Spectral phonon thermal properties in graphene nanoribbons, *Carbon* 93, 915 (2015)
27. R. Guo and B. Huang, Thermal transport in nanoporous Si: Anisotropy and junction effects, *Int. J. Heat Mass Transfer* 77, 131 (2014)
28. X. Yan, Y. Xiao, and Z. Li, Effects of intertube coupling and tube chirality on thermal transport of carbon nanotubes, *J. Appl. Phys.* 99(12), 124305 (2006)
29. D. Donadio and G. Galli, Thermal conductivity of isolated and interacting carbon nanotubes: Comparing results from molecular dynamics and the Boltzmann transport equation, *Phys. Rev. Lett.* 99(25), 255502 (2007)
30. Z. Ong, E. Pop, and J. Shiomi, Reduction of phonon lifetimes and thermal conductivity of a carbon nanotube on amorphous silica, *Phys. Rev. B* 84(16), 165418 (2011)
31. Z. Guo, D. Zhang, and X. Gong, Manipulating thermal conductivity through substrate coupling, *Phys. Rev. B* 84(7), 075470 (2011)
32. Z. Ong and E. Pop, Effect of substrate modes on thermal transport in supported graphene, *Phys. Rev. B* 84(7), 075471 (2011)
33. X. Zhang, H. Bao, and M. Hu, Bilateral substrate effect on the thermal conductivity of two-dimensional silicon, *Nanoscale* 7(14), 6014 (2015)
34. J. Yang, Y. Yang, S. Waltermire, X. Wu, H. Zhang, T. Gutu, Y. Jiang, Y. Chen, A. Zinn, R. Prasher, T. Xu, and D. Li, Enhanced and switchable nanoscale thermal conduction due to van der Waals interfaces, *Nat. Nanotechnol.* 7(2), 91 (2012)
35. O. Braun and Y. Kivshar, Nonlinear dynamics of the Frenkel–Kontorova model, *Phys. Rep.* 306(1), 1 (1998)
36. B. Hu and L. Yang, Heat conduction in the Frenkel–Kontorova model, *Chaos* 15(1), 015119 (2005)
37. L. Wang and B. Li, Thermal logic gates: Computation with phonons, *Phys. Rev. Lett.* 99(17), 177208 (2007)
38. L. Wang and B. Li, Thermal memory: A storage of phononic information, *Phys. Rev. Lett.* 101(26), 267203 (2008)
39. B. Hu, L. Yang, and Y. Zhang, Asymmetric heat conduction in nonlinear lattices, *Phys. Rev. Lett.* 97(12), 124302 (2006)
40. J. Wang and Z. G. Zheng, Heat conduction and reversed thermal diode: The interface effect, *Phys. Rev. E* 81(1), 011114 (2010)
41. E. Díaz, R. Gutierrez, and G. Cuniberti, Heat transport and thermal rectification in molecular junctions: A minimal model approach, *Phys. Rev. B* 84(14), 144302 (2011)
42. B. Q. Ai and B. Hu, Heat conduction in deformable Frenkel–Kontorova lattices: Thermal conductivity and negative differential thermal resistance, *Phys. Rev. E* 83(1), 011131 (2011)
43. W. R. Zhong, Different thermal conductance of the inter- and intrachain interactions in a double-stranded molecular structure, *Phys. Rev. E* 81(6), 061131 (2010)
44. B. Hu, D. He, Y. Zhang, and L. Yang, Asymmetric heat conduction in the Frenkel–Kontorova model,*Korean Phys. Soc.* 50, 166 (2007)
45. D. He, B. Ai, H. K. Chan, and B. Hu, Heat conduction in the nonlinear response regime: Scaling, boundary jumps, and negative differential thermal resistance, *Phys. Rev. E* 81(4), 041131 (2010)
46. J. Tekić, D. He, and B. Hu, Noise effects in the ac-driven Frenkel–Kontorova model, *Phys. Rev. E* 79(3), 036604 (2009)
47. J. Thomas, J. E. Turney, R. Iutzi, C. Amon, and A. McGaughey, Predicting phonon dispersion relations and lifetimes from the spectral energy density, *Phys. Rev. B* 81(8), 081411 (2010)
48. L. Zhu and B. Li, Low thermal conductivity in ultrathin carbon nanotube (2, 1), *Sci. Rep.* 4, 4917 (2014)
49. N. de Koker, Thermal conductivity of MgO periclase from equilibrium first principles molecular dynamics, *Phys. Rev. Lett.* 103(12), 125902 (2009)
50. S. Nosé, A molecular dynamics method for simulations in the canonical ensemble, *Mol. Phys.* 52(2), 255 (1984)
51. W. G. Hoover, Canonical dynamics: Equilibrium phase-space distributions, *Phys. Rev. A* 31(3), 1695 (1985)
52. W. H. Press, S. A. Teukolsky, W. T. Vetterling, and B. P. Flannery, Numerical Recipes, Cambridge: Cambridge University Press, 1992
53. A. V. Savin and O. V. Gendelman, Heat conduction in one-dimensional lattices with on-site potential, *Phys. Rev. E* 67(4), 041205 (2003)
54. C. Giardiná, R. Livi, A. Politi, and M. Vassalli, Finite thermal conductivity in 1D lattices, *Phys. Rev. Lett.* 84(10), 2144 (2000)
55. Q. W. Hou, B. Y. Cao, and Z. Y. Guo, Thermal conductivity of carbon nanotube: From ballistic to diffusive transport, *Acta Physica Sinica* 58(11), 7809 (2009) (in Chinese)
56. A. Jain, Y. J. Yu, and A. J. McGaughey, Phonon transport in periodic silicon nanoporous films with feature sizes greater than 100 nm, *Phys. Rev. B* 87(19), 195301 (2013)